P3 High Speed 3-D Wave Optical Simulation for Image Sensors

Hideki Mutoh
Link Research Corporation

1-18-5, Kojima, Taito-Ku, Tokyo, 111-0056 Japan
Phone: +81-3-3851-9871, FAX: +81-3-3862-0570, E-mail: hideki.mutoh@nifty.com

Abstract

A novel wave optical simulation method, localized boundary element method, has been developed. This method can execute 3-D wave optical simulation with much smaller memory space and much shorter calculation time than conventional boundary element method or finite difference time domain method. The accuracy and calculation speed of this method are discussed.

I. Introduction

Recently, the pixel size of image sensors has been steadily reduced. But it has been found that the small pixel size less than three micron causes some serious problems based on wave characteristics of the incident light, such as reduction of light gathering power of micro-lens and enhancement of color shading [3], [6]. The above phenomena cannot be treated by ray-tracing method. Therefore, we have been developing wave optical simulators, boundary element method (BEM) optical simulator TOCCATA-WAVE [1], [2] and finite difference time domain (FDTD) method optical simulator TOCCATA-FDTD [3]. Although these simulators are very useful and powerful tools to analyze wave optical characteristics, they have some difficulties in calculation time and required memory especially for 3-D wave optical analysis. Since the 3-D analysis becomes important with reduction of pixel size, high-speed 3-D wave optical simulator is strongly needed. Therefore, we have developed a new method, localized boundary element method (LBEM). The method can drastically reduce the calculation time and memory size. The comparison of calculation methods and color shading characteristics analyzed by this method are reported.

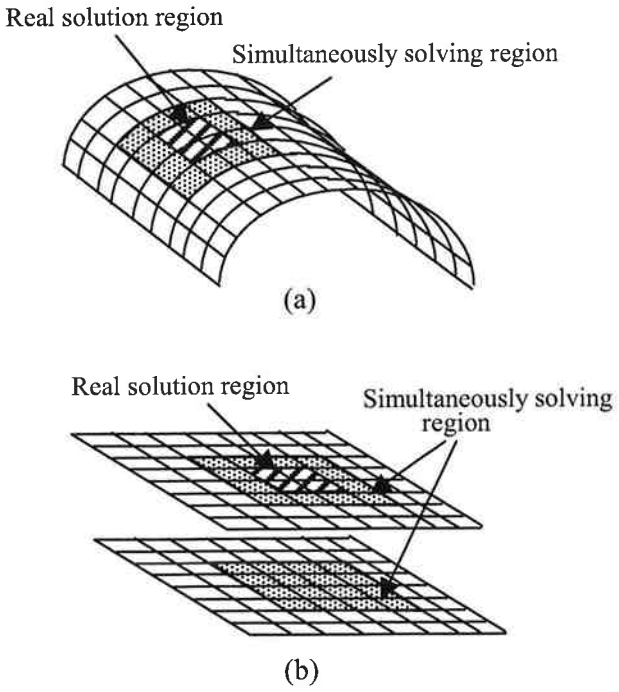

Fig. 1. Real solution and simultaneously solving region for localized boundary element method.
(a) Normal boundary. (b) Thin film boundary.

II. Calculation Model and method

Every component of electromagnetic field ϕ satisfies the following Helmholtz equation in the steady state condition.

$$\nabla^2\phi + k^2\phi = 0 \quad (1)$$

where k denotes the propagation number given as $2\pi/\lambda$ by wavelength λ. The above equation can be rewritten to the following integral equation by using Green function $G(\mathbf{x}, \mathbf{x}')$.

$$\phi(\mathbf{x}) = \oint_S \left[G(\mathbf{x},\mathbf{x}')\phi^*(\mathbf{x}') - G^*(\mathbf{x},\mathbf{x}')\phi(\mathbf{x}')\right] dS(\mathbf{x}') \quad (2)$$

S represents a closed surface surrounding the point

x, and * denotes differential operation along normal direction at **x'** on *S*. In three dimensional case, G(**x**,**x'**) is the following sphere wave function.

$$G(\mathbf{x},\mathbf{x}') = e^{ikr}/4\pi r \quad (3)$$

where

$$r = |\mathbf{x}-\mathbf{x}'| \quad (4)$$

The conventional boundary element method simultaneously solves electromagnetic field on all mesh points, considering the interaction among them. On the other hand, the localized boundary element method localizes the region where electromagnetic field is simultaneously solved and adopts that of the center region as the real solution by neglecting the peripheral region shown in Fig. 1 (a). The center region is shifted step by step, covering whole boundary surface. In the case of thin film multi layer structure, the above localized region is set on plural boundaries constructing the thin film as shown in Fig. 1 (b). This method drastically reduces memory size and calculation time compared with conventional boundary element method or finite difference time domain method.

III. Light gathering power dependence on cell size

Fig. 2 shows the structure for the analysis of micro-lens light gathering power dependence on cell size in the case of 25 % aperture ratio [3], [5]. The every length, the radius of sphere micro-lens, the distance between micro-lens and photo-sensitive plane, and aperture size of photo-sensitive region, is proportionally changed with cell size.

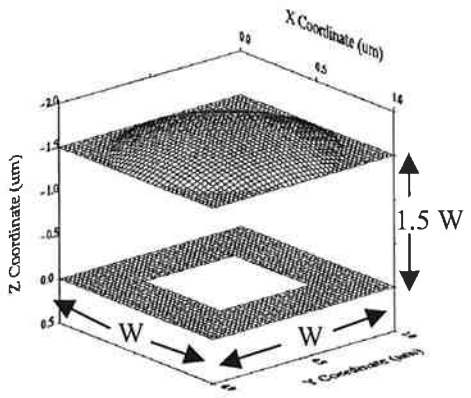

Fig. 2. Structure for wave optical simulation of light gathering power dependence on cell size. Center of the plane of Z=0 is the photo-sensitive region.

The light gathering power dependence on cell size by vertical incident light with wavelength of 550 nm is shown in Fig. 3. Although the figures show quite small difference among three methods, BEM, FDTD and LBEM, the required calculation time is extremely different among them, that is 30 hours for BEM, 15 hours for FDTD and 10 minutes for LBEM. LBEM is 10 to 100 times faster than BEM or FDTD.

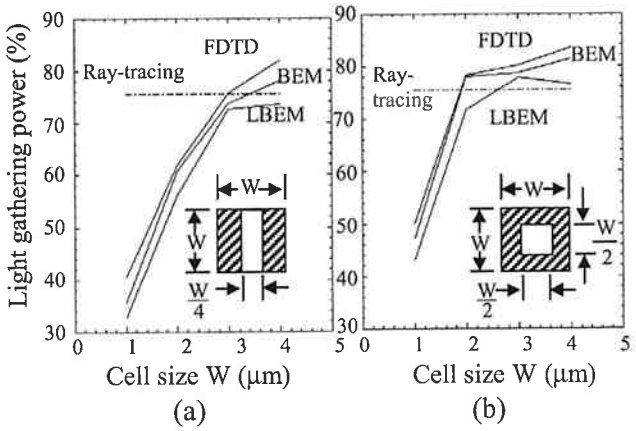

Fig. 3. Micro-lens light gathering power dependence on cell size by 550 nm vertical incident light for rectangular (a) and square (b) photo- sensitive region with 25 % aperture ratio.

IV. Reflectance of multi-layer structure

The multi-layer structure, $SiO_2/Si_3N_4/SiO_2/Si$, is often utilized for the purpose of anti-reflection [4]. Fig. 4 shows the comparison of reflectance in the above thin film multi-layer structure between 2-D LBEM and analytical 1-D calculation. It is found that the reflectance dependence on wavelength obtained by LBEM is nearly same as analytical 1-D calculation. LBEM can treat interference of thin film with reasonable accuracy.

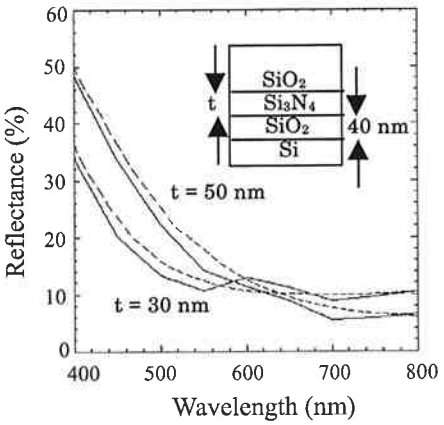

Fig. 4. Reflectance dependence on wavelength and Si_3N_4 thickness in $SiO_2/Si_3N_4/SiO_2/Si$ structure. Broken line: 1-D analysis, solid line: LBEM. Bottom SiO_2 thickness is 40 nm.

V. Color shading characteristics

The color shading is one of the most serious problems for small size image sensors, because focal region has finite width to be nearly proportional to wavelength [6]. Although the center pixel can receive most of the light power even for long wavelength incident light, the peripheral pixel loses larger part of the power for the longer wavelength light, because the peripheral pixel receives oblique incident light. Fig. 5 shows the vertical cross-section of 3-D structures for the color shading analysis with single (a), double (b), and triple (c) micro-lenses.

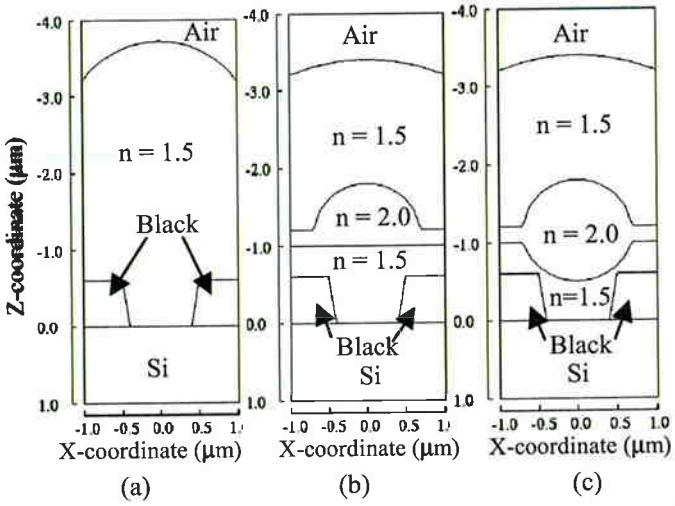

Fig. 5. Structures for the analysis of color shading characteristics dependence on cell size. (a) Single lens structure. (b) Double lens structure. (c) Triple lens structure. "n" denotes refractive index of the material.

Fig. 6 and 7 show the light intensity distribution of peripheral pixel in the three structures with wavelength of 400 nm and 700 nm, respectively. Top lenses of three structures are shifted proportionally with the distance between the chip center and the pixel position. Since the single lens structure has largest width and largest lateral shift of the focal region, the light gathering power loss is largest among the three structures. On the other hand, the triple lens structure has smallest loss of the light gathering power, because of the smallest width and smallest lateral shift of the focal region. Comparing Fig.6 and 7, it is found that the light gathering power loss in the longer wavelength case is larger than that in the smaller wavelength case, because the longer wavelength light gives the wider focal region.

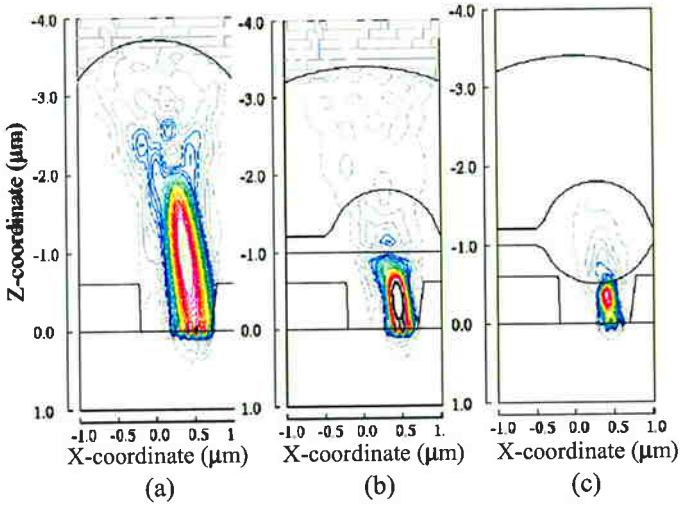

Fig. 6. Light intensity distribution of peripheral pixel with wavelength of 400 nm in 2 μm square pixel. (a) Single lens structure. (b) Double lens structure. (c) Triple lens structure. The top lenses are shifted with 0.14 times length of cell size. The incident light angle is 12 degree.

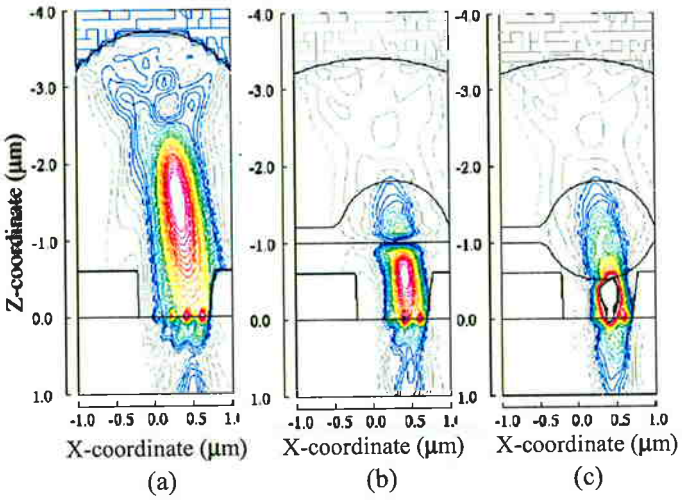

Fig. 7. Light intensity distribution of peripheral pixel with wavelength of 700 nm in 2 μm square pixel. (a) Single lens structure. (b) Double lens structure. (c) Triple lens structure. The top lenses are shifted with 0.14 times length of cell size. The incident light angle is 12 degree.

Fig. 8 shows the calculation result of the light gathering power dependence on cell size, wavelength, and pixel position. Comparing the three structures, the triple lens structure has the most stable light gathering power for the fluctuation of cell size or incident light angle. The triple lens structure seems to be the best among the three structures for color shading characteristics.

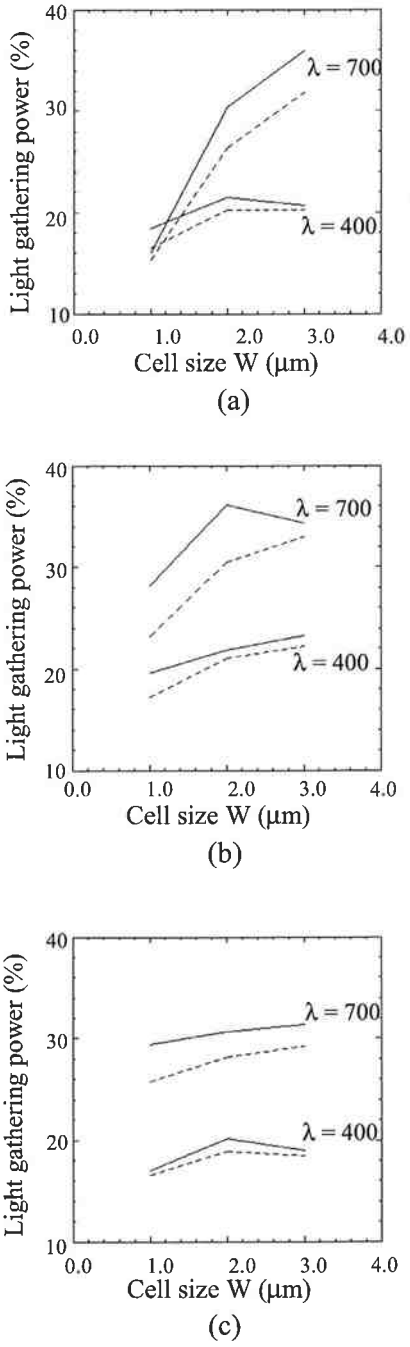

Fig. 8. Light gathering power dependence on cell size by the incident light wavelength of 400 nm and 700 nm. Solid line and broken line denote the light gathering power of center pixel and peripheral pixel, respectively. (a) Single lens structure. (b) Double lens structure. (c) Triple lens structure.

VI. Comparison among calculation methods

Table 1 shows the comparison among BEM, FDTD, and LBEM. The calculation time and required memory size is proportional to $W^4 L^2/\lambda^4$ for BEM, W^3/λ^3 for FDTD, and W^2L/λ^2 for LBEM, where W, L, and λ denote cell size, total layer number, and wavelength, respectively. LBEM realizes 3-D wave optical simulation with very small memory space and extremely short calculation time.

Table 1. Comparison among BEM, FDTD, and LBEM

	BEM	FDTD	LBEM
Total Array Size	$W^4 L^2/\lambda^4$	W^3/λ^3	$W^2 L/\lambda^2$
Accuracy	Excellent	Good	Good
Calculation Time	No good	Good	Excellent
Required Memory	No good	Good	Excellent
Angle Dependence	Excellent	No good	Good

W: Cell size, L: Total layer number, λ: Wavelength

VII. Conclusion

It was found that the localized boundary element method is much faster than conventional method and its result has reasonable accuracy. It would be a powerful tool to design and analyze small pixel image sensor structures, including light gathering power and color shading characteristics.

VIII. Acknowledgment

The author would like to thank Dr. T. Yamada, Mr. M. Shizukuishi, and Mr. S. Uya of Fuji Photo Film Co., Ltd. for their helpful discussion about the color shading characteristics.

References

[1] H. Mutoh, "Simulation for 3-dimensional optical and electrical analysis of CCD," *IEEE Trans. Electron D evices*, vol. 44, pp. 1604-1610, Oct. 1997.

[2] H. Mutoh, "Optical simulation for image sensors by wave analysis," Proceeding of 1997 IEEE Workshop on CCD and AIS, 1997.

[3] H. Mutoh, "3-D Optical and Electrical Simulation for CMOS Image Sensors," Proceeding of 2003 IEEE Workshop on CCD and AIS, 2003.

[4] I. Murakami, et. al., "Technologies to improve photo-sensitivity and reduce VOD shutter voltage for CCD image sensors," *IEEE Trans. Electron Devices*, vol. 47, pp. 1566-1572, Aug. 2000.

[5] H. Mutoh, "3-D wave optical simulation of inner-layer lens structures," Proceeding of 1999 IEEE Workshop on CCD and AIS, 1999.

[6] H. Mutoh, et. al., "Wave optical simulation for CCD color shading," Proceeding of ITE Annual Convention 2004, 13-7, 2004.